ChemComm

COMMUNICATION

View Article Online
View Journal | View Issue

Cite this: *Chem. Commun.*, 2024, **60**, 14049

Received 20th September 2024,
Accepted 4th November 2024

DOI: 10.1039/d4cc04651j

rsc.li/chemcomm

Alkenylation of unactivated alkanes: synthesis of *Z*-alkenes *via* dual Co-TBADT catalysis†

Vetrivelan Murugesan, Anagha Syam, Guru Vigknesh Anantharaj and Ramesh Rasappan *

Hydroalkylation of terminal alkynes *via* C–H activation is the most atom-economical and straightforward method for synthesizing alkenes. They remain confined to using C(sp^2)–H or activated C(sp^3)–H bonds. A chelating group enabled the alkenylation of C(sp^3)–H bonds, resulting in *E* alkenes. Protocols by which alkenylation of unactivated C(sp^3)–H bonds occurs without a chelating group *via* metal-hydride or radical pathways remain unknown. Our cobalt-HAT catalysis achieves the desired *Z* alkene with excellent regio- and diastereoselectivity *via* C–H activation.

In organic synthesis, alkenes serve as versatile and unique building blocks.[1] Among the numerous methods that exist, transition metal catalyzed hydroalkylation[2] of readily available terminal alkynes is regarded as one of the most versatile methods for the stereo- and regio-controlled synthesis of alkenes. The direct addition of a C–H bond across an alkyne is notably the most atom- and step-economical method.[3] Despite notable advancements in the utilization of C(sp^2)–H and activated C(sp^3)–H bonds for hydroalkylation,[4] unactivated C(sp^3)–H bonds are seldom encountered, necessitating the presence of a chelating group, and are predominantly employed with internal alkynes (Scheme 1b).[5]

Transition metal-mediated hydroalkylation *via* C–H activation typically yields *syn*-adducts by concerted metalation–deprotonation (CMD) or metal-hydride routes (Scheme 1a). Conversely, the alternate approach of adding carbon-centred radicals to alkynes results in limited stereoselectivity[6] owing to the *in situ* formation of vinyl radicals with either π (linear) or σ (bent and rapidly inverting) geometry.[7] The vinyl radical, fortunately, generates configurationally stable vinyl-metal species *in situ*,[8] which have been utilized successfully in stereospecific transformations.[9]

Although radical additions to alkenes have been extensively studied,[10] additions to alkynes are less prevalent (Scheme 1c).[6b,11] This can be attributed to the higher singlet–triplet energy gap and/or the generation of a highly reactive intermediate vinyl radical.[7b,12] On the other hand, photocatalysis has been effectively employed to synthesize alkenes through HAT processes.[13] Employing Ni/Ir dual catalysis, the group of Macmillan[9b] and Rueping[9c] recently revealed a decarboxylative hydroalkylation (Scheme 1d). There are currently no known methods for accommodating unactivated alkanes in hydroalkylation in the absence of chelating groups *via* radical additions, metal hydride, or CMD. Herein, we demonstrate the application of cobalt-HAT catalysis in generating the desired *Z* alkene with high regio- and diastereoselectivity.

We commenced our study with substrates 1-(*tert*-butyl)-4-ethynylbenzene **1a** and cyclohexane **2a**. Under the optimized

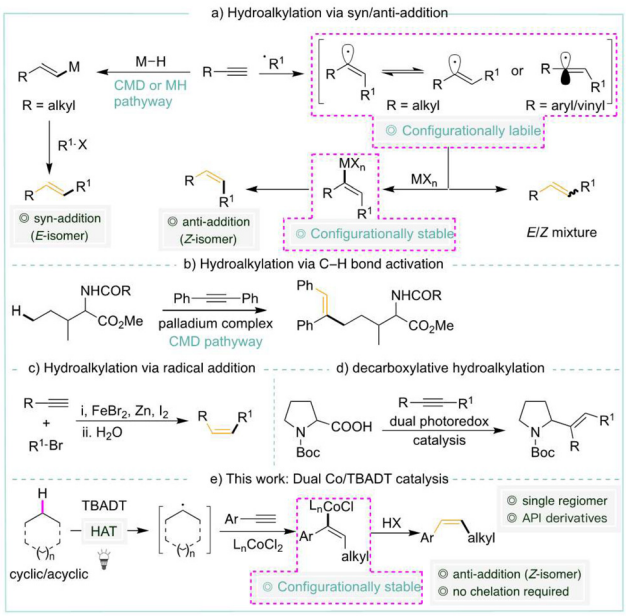

Scheme 1 Hydroalkylation of alkynes.

School of Chemistry, Indian Institute of Science Education and Research Thiruvananthapuram, Vithura, Thiruvananthapuram, Kerala 695551, India. E-mail: rr@iisertvm.ac.in

† Electronic supplementary information (ESI) available. See DOI: https://doi.org/10.1039/d4cc04651j

Table 1 Optimization of the reaction conditions[a]

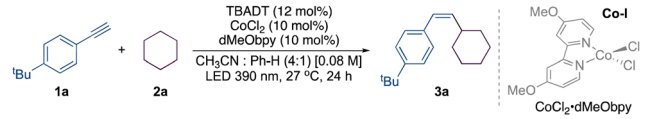

Entry	Deviation from above	1a[b]	3a[b] (Z:E)
1[c]	(7.5 mol%) $NiCl_2$·dtbpy	n.d.	37 (79:21)
2[c]	(7.5 mol%) $NiBr_2$·phen	n.d.	40 (80:20)
3	(10 mol%) $CoCl_2$, phen	25	60 (80:20)
4	(10 mol%) $CoCl_2$, tMephen	29	48 (81:19)
5	(10 mol%) $CoCl_2$, dMebpy	23	61 (79:21)
6	No deviation	15	74 (84:16)
7	(10 mol%) $CoCl_2$, dtbpy	18	68 (87:13)
8	(10 mol%) $CoCl_2$, (20 mol%) dmap	19	32 (82:18)
9	(10 mol%) PC, (10 mol%) **Co-I**	*T*	89 (80:20)
10	(5 mol%) PC, (10 mol%) **Co-I**	27	71 (90:10)
11	Same as entry 10, 60 h	9	80 (91:9)
12	Same as entry 10, acetone (0.08 M)	88	5 (75:25)
13	Same as entry 10, DMSO (0.08 M)	91	<5
14	(5 mol%) PC, (5 mol%) **Co-I**	22	58 (80:20)
15	(7.5 mol%) PC, (15 mol%) **Co-I**	6	93 (86:14)
16	(7.5 mol%) PC, (23 mol%) **Co-I**	6	87 (92:8)
17	(5 mol%) PC, (20 mol%) **Co-I**	25	73 (95:5)
18[a]	(4 + 2 mol%) PC, (16 + 4 mol%) **Co-I**	<5	**83 (93:7)**[d]
19	Same as entry 15, 25 eq. of CyH	42	37 (90:10)
20[e]	(30 mol%) An added as sensitizer	32	55 (91:9)
21[e]	(20 mol%) BP added as sensitizer	38	43 (85:15)
22	Without TBADT or $CoCl_2$·dMeObpy[f]	99	n.d.
23[a]	Under air	15	51 (89:11)
24[a]	20 eq. H_2O added	10	47 (85:15)

[a] Optimized conditions: 0.15 mmol of **1a**, 7.5 mmol of **2a**, 6 mol% of PC – TBADT (portion wise), 20 mol% of **Co-I** (portion wise), CH_3CN:PhH (4:1, 0.08 M), 390 nm, 27 °C, 48 h. [b] Determined by ^1H NMR using 1,3,5-trimethoxybenzene as an internal standard. [c] CH_3CN [0.1 M]. [d] Isolated yields. [e] 5 mol% of TBADT. [f] 7.5 mol% of TBADT; bpy – 2,2′-bipyridine; phen – 1,10-phenanthroline; dMeObpy – 4,4′-dimethoxy-2,2′-bipyridine; dMebpy – 4,4′-dimethyl-2,2′-bipyridine; dtbpy – 4,4-di-*tert*-butyl-2,2-dipyridyl; tMephen – 3,4,7,8-tetramethyl-1,10-phenanthroline.

conditions involving 20 mol% $CoCl_2$ and 6 mol% TBADT, **3a** was obtained in 83% isolated yield with a ratio of 93:7 (*Z*:*E*) (entry 18). A comprehensive selection of nickel complexes was evaluated in light of our prior expertise in dual TBADT-nickel catalysis (Table S1, ESI†).[14] Nevertheless, when $NiCl_2$·dtbpy and $NiBr_2$·phen were utilized, the cross-coupled product **3a** was obtained only in 37% and 40% yield (Table 1, entries 1 and 2), respectively, with a moderate *Z*:*E* ratio. Significantly, the majority of entries utilizing a nickel complex exhibited complete consumption of alkyne **1a** (Table S1, ESI†). Pleasingly, a dramatic improvement in the yield was observed when $CoCl_2$ was employed (Table S3, ESI†). Additionally, in order to augment the reaction, a variety of ligands (Table 1, entries 3–8) were utilized, comprising phen, tMephen, dMebpy, and dtbpy (Table 1, entries 3–5 and 7). Of the several ligands that were evaluated, those based on bipyridine demonstrated an enhanced yield for the synthesis of **3a**. In particular, ligand dMeObpy produced **3a** with a 74% yield (entry 6). The moderate yields were attributable to an incomplete consumption of alkyne **1a**. Having identified the optimal ligand, reactions were conducted by altering the catalyst loadings. A significant improvement in yield was observed when the precomplexed cobalt catalyst was used with decreased loading of TBADT (Table 1, entry 9).

A further decrease in the loading of TBADT from 12 mol% to 5 mol% was shown to have a negative impact (Table 1, entry 10). No reaction was visually discernible in DMSO or acetone (Table 1, entries 12 and 13). The ideal reaction conditions necessitate the utilization of a 4:1 mixture of CH_3CN:PhH. None of the alternative solvents that were evaluated (Table S2, ESI†) proved to be effective. Consequently, our study focused on altering the proportion between TBADT and $CoCl_2$, as well as adjusting the loading of the catalyst (Table 1, entries 14–17). While 7.5% TBADT increased the yield of **3a**, it also decreased the *Z*:*E* ratio of **3a** to 86:14 (Table 1, entry 15). Control experiments conducted in the absence of TBADT or $CoCl_2$·dMeObpy demonstrate the indispensability of these particular reagents (Table 1, entry 22). The yield of **3a** was diminished when the quantity of cyclohexane was reduced (Table 1, entry 19). Photosensitizers are recognized for their ability to promote *E* to *Z* isomerization.[15] However, the use of photosensitizers such as anthracene (An) and benzophenone (BP) did not prove beneficial in enhancing the *E*/*Z* ratio (entries 20 and 21). The reaction can be performed at 4 mmol scale; the complete consumption of **1a** necessitated 5 days, resulting in the isolation of **3a** with a yield of 70% (*Z*:*E* – 92:8) (SI-21, ESI†).

Table 2 depicts the scope of alkynes and alkanes. Phenyl acetylenes incorporating *tert*-butyl, methyl, ethyl, phenyl, and π-extended naphthyl groups exhibited efficient cross-coupling reactions. The aryl bromides (**1g** and **1h**) and chlorides (**1i** and **1j**) remained intact. The medicinally significant fluoro and trifluoromethyl derivatives **1k** and **1l** were synthesized with respective yields of 73% and 70%. The compatibility of the methyl and phenyl ethers **1m–1p** was also demonstrated. Pleasingly, no competing reactions involving esters and ketones were observed. The nitrile group was likewise compatible. We employed heterocycles including thiophene and indole derivatives **1t–1v** under the optimized conditions. Consequently, high yields of the corresponding coupled products **3t–3v** were effectively obtained. Remarkably, the Boc protecting group, known for its high sensitivity, remained stable throughout the reaction. Equally striking was the compatibility of the unprotected amine; indole **1v** and aniline **1w** produced **3v** and **3w** in 60% and 49% isolated yields, respectively. Perhaps importantly, the compatibility of the boronic ester ensured that subsequent functionalization remained viable. In addition, the MOM group **3y**, which is particularly sensitive to acid, remained stable under the optimized reaction conditions. Furthermore, the scope of alkanes **2** was expanded. Cycloheptane and cyclooctane were compatible, producing **3aa** and **3ab** in satisfactory yields, as predicted. Acyclic alkanes were also found to be compatible, yielding a mixture of isomers. We also illustrate the effectiveness of the approach in instances of polarity-matched and mismatched HATs. As anticipated, the polarity-matched α-heteromethylenes underwent successful functionalization to yield the corresponding alkenes **3ae–3ag**. The polarity-mismatched α-methylenes in carbonyl compounds were intact; as demonstrated in Table 2, cyclopentanone and

Table 2 Scope for alkenylation of unactivated alkanes[a]

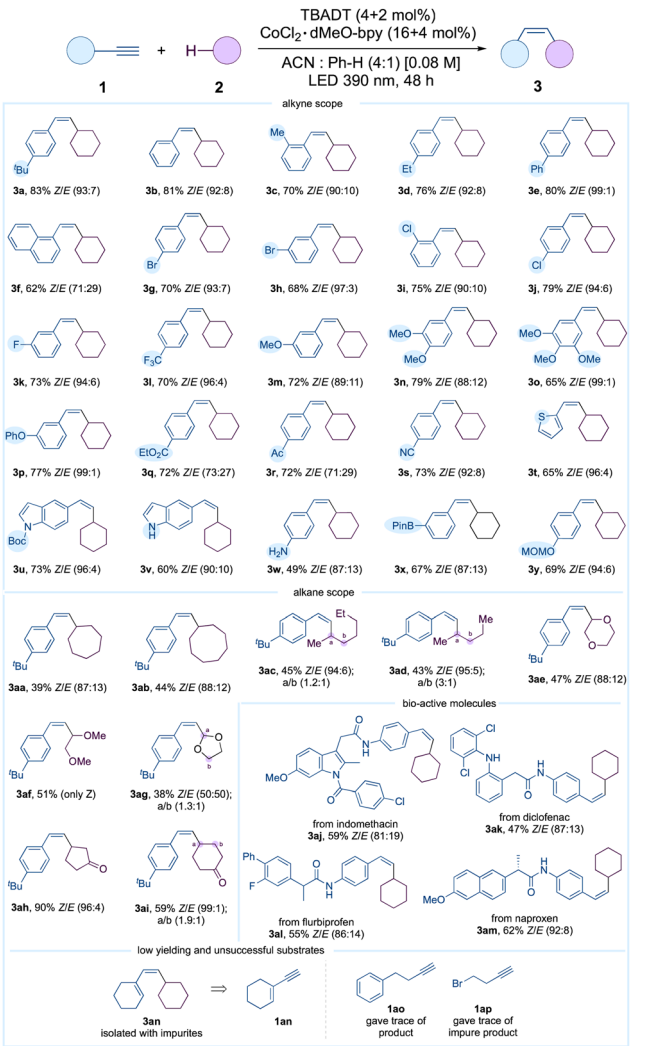

cyclohexanone exhibited compatibility and produced the cross-coupled products **3ah** and **3ai** with good yields. The API derivatives; indomethacin **3aj**, diclofenac **3ak**, flurbiprofen **3al**, and naproxen **3am** derivatives were obtained with satisfactory yields. Of note, when the enyne **1an** was employed, a mixture of impure products was obtained. The alkyl alkynes including but-3-yn-1-ylbenzene **1ao** and 4-bromobut-1-yne **1ap** were recovered intact. Regrettably, *N*-methylmorpholine, *N*-methylpyrrolidine, and tetrahydrothiophene did not yield the coupled product. It is interesting that the formation of **3a** was entirely suppressed when 2 eq. of *N*-methylmorpholine was added to the default reaction (SI-87, ESI†).

The introduction of deuterated methanol under the optimized reaction conditions led to a 70% incorporation of deuterium in the cross-coupled product **3a-D**. Utilizing deuterated aryl acetylene **1m-D**, we identified 100% deuterium incorporation in the product **3m-D**. These results rule out the potential for aryl acetylide to serve as an intermediate. NMR analysis of the reaction crude in the presence of TEMPO revealed the presence of the TEMPO adduct **4**, confirming

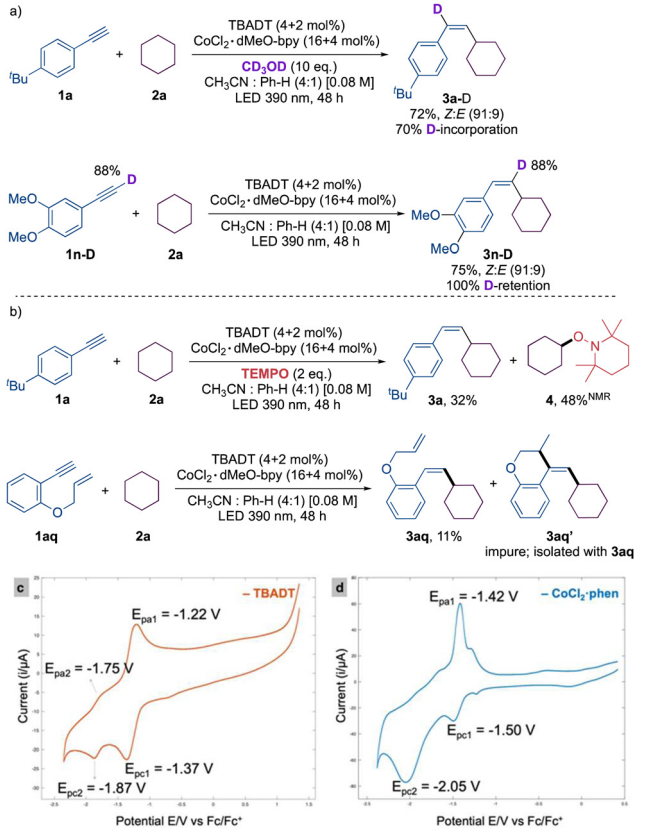

Scheme 2 (a) Deuterium labelling experiments, and (b) radical trap experiments. Cyclic voltammogram of (c) TBADT and (d) $CoCl_2$·1,10-phenanthroline.

cyclohexyl radical intermediacy. Additionally, radical clock substrate **1aq** offered the cyclized product **3aq′** in conjunction with uncyclized product **3aq**, which confirms the presence of a vinyl radical intermediate (Scheme 2).

A cyclic voltammogram was conducted to gain a more comprehensive understanding of the mechanism, as we anticipated that the effective reducing agent would be $[W_{10}O_{32}]^{6-}$ rather than $[W_{10}O_{32}]^{5-}$.[16] The cyclic voltammetry (CV) of TBADT showed two chemically reversible reductions at potentials of −1.37 V and −1.87 V, which correspond to the reduction of $[W_{10}O_{32}]^{4-}/[W_{10}O_{32}]^{5-}$ and $[W_{10}O_{32}]^{5-}/[W_{10}O_{32}]^{6-}$, respectively. In contrast to the irreversible reduction peak observed in the CV of the default complex, Co(II)Cl_2·dMeObpy (**Co-I**), an equally effective complex, $CoCl_2$·phen (entry 5, Table S4, ESI†), displayed two subsequent reductions. The reversible peak at −1.5 V is presumably assigned to Co(II)/Co(I) and the irreversible peak at −2.05 V is assigned to Co(I)/Co(0).[17] Given that the reduction potential of $[W_{10}O_{32}]^{4-}/[W_{10}O_{32}]^{5-}$ is more anodic than that of Co(II) to Co(I), it is probable that $[W_{10}O_{32}]^{6-}$ reduces the Co(II) complex. Furthermore, as the reduction of Co(I) to Co(0) happens at a more cathodic potential, the active low valence species is attributed to the Co(I) species.

Based on our prior[14,16b] and current studies, we postulated a hypothetical mechanism in Scheme 3. The catalytic cycle begins when the 390 nm LED excites TBADT (LMCT

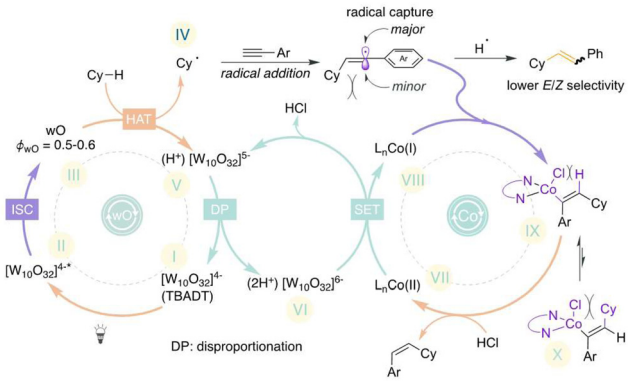

Scheme 3 Hypothetical mechanism.

(ligand-to-metal charge transfer): oxygen → tungsten), resulting in the short-lived excited species $[W_{10}O_{32}]^{4-*}$. Subsequent intersystem crossing generates the long-lived triplet wO species, which undertakes a HAT event to produce the alkyl radical **IV** and pentavalent decatungstate, $[W_{10}O_{32}]^{5-}$. The pentavalent decatungstate undergoes disproportionation, resulting in the regeneration of $[W_{10}O_{32}]^{4-}$ and the emergence of the strong reductant $[W_{10}O_{32}]^{6-}$. This reductant then reduces the Co(II) complex **VII**, generating the low-valent Co(I) complex **VIII**. In parallel, the alkyl radical that is *in situ*-generated is captured by an alkyne, resulting in the formation of a thermodynamically unstable transitory vinyl radical. Ultimately, the vinyl radical is captured by the low valent Co(I) complex **VIII** in a stereoselective manner or the generated species **IX** is more favourable than **X** because the cyclohexyl group and the ligands attached to the cobalt center exhibit steric hinderance in X. Following this, the vinyl cobalt intermediate is protodemetallated in order to generate the desired alkene product and restore the Co(II) complex **VII**. The alternate pathway wherein the alkyl radical (IV) combines with Co(I) and subsequently undergoes hydroalkylation is excluded as it would result in the formation of the *E*-isomer.

In conclusion, a protocol was developed to facilitate the hydroalkylation of terminal alkynes through the C–H activation of unactivated cyclic/acyclic alkanes. The inclusion of sensitive functional groups like carbonyl, nitrile, and Bpin as well as acid-sensitive groups like MOM and Boc demonstrates the mitigation of the reaction conditions. The scope of alkanes was broadened to include acyclic alkanes and APIs. A mechanism has been disclosed by preliminary mechanistic investigations.

We thank IISER Trivandrum and Science and Engineering Research Board; CRG/2023/005485 and RSC Research Fund grant; R23-8225379124 for the financial support. A. S. acknowledges CSIR. V. M. acknowledges IISER Trivandrum for the fellowship.

Data availability

The data supporting this article have been included as part of the ESI.†

Conflicts of interest

There are no conflicts to declare.

Notes and references

1 (*a*) A. Flynn and W. Ogilvie, *Chem. Rev.*, 2007, **107**, 4698; (*b*) C. Oger, L. Balas, T. Durand and J. Galano, *Chem. Rev.*, 2013, **113**, 1313.
2 (*a*) X. Lu, J. Liu, X. Lu, Z. Zhang, T. Gong, B. Xiao and Y. Fu, *Chem. Commun.*, 2016, **52**, 5324; (*b*) A. Suess, M. Uehling, W. Kaminsky and G. Lalic, *J. Am. Chem. Soc.*, 2015, **137**, 7747.
3 (*a*) Y. Minami and T. Hiyama, *Acc. Chem. Res.*, 2016, **49**, 67; (*b*) L. Yang and H. Huang, *Chem. Rev.*, 2015, **115**, 3468; (*c*) K. Gao and N. Yoshikai, *Acc. Chem. Res.*, 2014, **47**, 1208.
4 (*a*) L. Ackermann, *Acc. Chem. Res.*, 2014, **47**, 281; (*b*) B. Zhou, H. Chen and C. Wang, *J. Am. Chem. Soc.*, 2013, **135**, 1264; (*c*) N. Chernyak, S. I. Gorelsky and V. Gevorgyan, *Angew. Chem., Int. Ed.*, 2011, **50**, 2342.
5 (*a*) Y. Nakao, E. Morita, H. Idei and T. Hiyama, *J. Am. Chem. Soc.*, 2011, **133**, 3264; (*b*) C. Lin, Z. Chen, Z. Liu and Y. Zhang, *Org. Lett.*, 2017, **19**, 850; (*c*) S. Maity, S. Agasti, A. Earsad, A. Hazra and D. Maiti, *Chem. – Eur. J.*, 2015, **21**, 11320; (*d*) M. Li, Y. Yang, D. Zhou, D. Wan and J. You, *Org. Lett.*, 2015, **17**, 2546; (*e*) J. Xu, Z. Zhang, W. Rao and B. Shi, *J. Am. Chem. Soc.*, 2016, **138**, 10750.
6 (*a*) Y. Zhang, L. Huang, K. Cheng, B. Yao and J. Zhao, *Synthesis*, 2009, 3504; (*b*) S. Feng, X. Xie, W. Zhang, L. Liu, Z. Zhong, D. Xu and X. She, *Org. Lett.*, 2016, **18**, 3846; (*c*) W. Chen, M. Zhang and Y. Zhao, *Synthesis*, 2016, 1342; (*d*) J. Li, J. Zhang, H. Tan and D. Wang, *Org. Lett.*, 2015, **17**, 2522.
7 (*a*) T. P. M. Goumans, K. van Alem and G. Lodder, *Eur. J. Org. Chem.*, 2008, 435; (*b*) U. Wille, *Chem. Rev.*, 2013, **113**, 813.
8 J. M. Huggins and R. G. Bergman, *J. Am. Chem. Soc.*, 1981, **103**, 3002.
9 (*a*) C. Cheung, F. Zhurkin and X. Hu, *J. Am. Chem. Soc.*, 2015, **137**, 4932; (*b*) N. Till, R. Smith and D. MacMillan, *J. Am. Chem. Soc.*, 2018, **140**, 5701; (*c*) H. Yue, C. Zhu, R. Kancherla, F. Liu and M. Rueping, *Angew. Chem., Int. Ed.*, 2020, **59**, 5738.
10 A. Capacci, J. Malinowski, N. McAlpine, J. Kuhne and D. MacMillan, *Nat. Chem.*, 2017, **9**, 1073.
11 (*a*) M. Huang, W. Hao, G. Li, S. Tu and B. Jiang, *Chem. Commun.*, 2018, **54**, 10791; (*b*) H. Han, Y. Lee, Y. Jung and S. Han, *Org. Lett.*, 2017, **19**, 1962; (*c*) H. Liang, Y. Ji, R. Wang, Z. Zhang and B. Zhang, *Org. Lett.*, 2019, **21**, 2750; (*d*) N. Chalotra, A. Ahmed, M. Rizvi, Z. Hussain, Q. Ahmed and B. Shah, *J. Org. Chem.*, 2018, **83**, 14443; (*e*) M. Alkan-Zambada and X. Hu, *J. Org. Chem.*, 2019, **84**, 4525.
12 (*a*) R. Gómez-Balderas, M. L. Coote, D. J. Henry, H. Fischer and L. Radom, *J. Phys. Chem. A*, 2003, **107**, 6082; (*b*) B. Giese and S. Lachhein, *Angew. Chem., Int. Ed.*, 1982, **21**, 768.
13 (*a*) K. Ohmatsu and T. Ooi, *Nat. Synth.*, 2023, **2**, 209; (*b*) Z. Ye, Y. Yu, Y.-M. Lin, Y. Chen, S. Song and L. Gong, *Nat. Synth.*, 2023, **2**, 766; (*c*) H. Cao, Y. Kuang, X. Shi, K. L. Wong, B. B. Tan, J. M. C. Kwan, X. Liu and J. Wu, *Nat. Commun.*, 2020, **11**, 1956; (*d*) M.-J. Zhou, L. Zhang, G. Liu, C. Xu and Z. Huang, *J. Am. Chem. Soc.*, 2021, **143**, 16470.
14 (*a*) V. Murugesan, A. Muralidharan, G. Anantharaj, T. Chinnusamy and R. Rasappan, *Org. Lett.*, 2022, **24**, 8435; (*b*) V. Murugesan, A. Ganguly, A. Karthika and R. Rasappan, *Org. Lett.*, 2021, **23**, 5389.
15 T. Neveselý, M. Wienhold, J. J. Molloy and R. Gilmour, *Chem. Rev.*, 2021, **122**, 2650.
16 (*a*) I. Perry, T. Brewer, P. Sarver, D. Schultz, D. DiRocco and D. MacMillan, *Nature*, 2018, **560**, 70; (*b*) R. Pilli, K. Selvam, B. S. S. Balamurugan, V. Jose and R. Rasappan, *Org. Lett.*, 2024, **26**, 2993; (*c*) X. Hu, I. Cheng-Sánchez, W. Kong, G. A. Molander and C. Nevado, *Nat. Catal.*, 2024, **7**, 655–665.
17 D. P. Hickey, C. Sandford, Z. Rhodes, T. Gensch, L. R. Fries, M. S. Sigman and S. D. Minteer, *J. Am. Chem. Soc.*, 2019, **141**, 1382.

